

# The importance of Icelandic ice sheet growth and retreat on mantle CO<sub>2</sub> flux

John J. Armitage<sup>1</sup>, David J. Ferguson<sup>2</sup>, Kenni D. Petersen<sup>3</sup>, and Timothy T. Creyts<sup>4</sup>

<sup>1</sup>Dynamique des Fluides Géologiques, Institut de Physique du Globe de Paris, Paris, France

<sup>2</sup>School of Earth and Environment, University of Leeds, Leeds, U.K.

<sup>3</sup>Department of Geoscience, University of Aarhus, Aarhus, Denmark

<sup>4</sup>Lamont-Doherty Earth Observatory, Columbia University, U.S.A

## Key Points:

- We combine a new history of Icelandic ice-cover with a forward model of magma generation.
- Magmatism and CO<sub>2</sub> outgassing is influenced by both the rate of deglaciation and, importantly, the preceding growth of the ice sheet.
- Peak mantle CO<sub>2</sub> flux is non-linearly related to magmatic eruption rates.

15 **Abstract**

16 Climate cycles may significantly affect the eruptive behavior of terrestrial volcanoes due  
 17 to pressure changes caused by glacial loading, which raises the possibility that climate  
 18 change may modulate CO<sub>2</sub> degassing via volcanism. In Iceland, magmatism is likely to  
 19 have been influenced by glacial activity. To explore if deglaciation therefore impacted  
 20 CO<sub>2</sub> flux we coupled a model of glacial loading over the last ~120 ka to melt generation  
 21 and transport. We find that a nuanced relationship exists between magmatism and glacial  
 22 activity. Enhanced CO<sub>2</sub> degassing happened prior to the main phase of late-Pleistocene  
 23 deglaciation, and it is sensitive to the duration of the growth of the ice sheet entering  
 24 into the LGM, as well as the rate of ice loss. Ice sheet growth depresses melting in the  
 25 upper mantle, creating a delayed pulse of CO<sub>2</sub> out-gassing as the magmatic system re-  
 26 covers from the effects of loading.

27 **1 Introduction**

28 Evidence from several tectonic settings indicates that glaciated volcanic systems  
 29 respond to changing ice volumes (Glazner, Manley, Marron, & Rojstaczer, 1999; Jellinek,  
 30 Mange, & Saar, 2004; Jull & McKenzie, 1996; MacLennan, Jull, McKenzie, Slater, & Grönvöld,  
 31 2002; Rawson et al., 2016; Sigvaldsson, Annertz, & Nilsson, 1992), and suggests there was  
 32 a widespread volcanic response to late-Pleistocene ice retreat (Huybers & Langmuir, 2009).  
 33 The most compelling evidence for climate-coupled volcanism comes from Iceland, where  
 34 changes in early Holocene lava volumes and magma chemistry are consistent with de-  
 35 pressurization during glacial unloading (Jull & McKenzie, 1996; MacLennan et al., 2002;  
 36 Sinton, Grönvöld, & Saemundsson, 2005). Magma generation here occurs due to pressure-  
 37 release melting, as the mantle up-wells beneath rift zones. Although the net change in  
 38 overburden pressures from variations in ice cover have been relatively small, the high rates  
 39 of change associated with glacial activity can produce significant short-term fluctuations  
 40 in magmatic output (Jull & McKenzie, 1996; Pagli & Sigmundsson, 2008; Schmidt et al.,  
 41 2013), similar to those hypothesised to occur at ocean ridges due to sea-level variation  
 42 (Burley & Katz, 2015; Crowley, Katz, Huybers, Langmuir, & Park, 2015; Huybers & Lang-  
 43 muir, 2009; Lund & Asimow, 2011). Carbon readily partitions into magmas during par-  
 44 tial melting (Rosenthal, Hauri, & Hirschmann, 2015) and is released as a CO<sub>2</sub> rich fluid/vapour  
 45 as the magma ascends through the crust, making volcanism the primary pathway for trans-  
 46 porting carbon from the Earth's mantle to the atmosphere (Dasgupta & Hirschmann,  
 47 2010). However, carbon does not enter the melt uniformly during partial melting and  
 48 is concentrated in early formed magma. Therefore the extent to which glacially driven  
 49 changes in primary magma generation alter the flux of CO<sub>2</sub> depends on where in the melt-  
 50 ing column melt production is enhanced (or suppressed), the rate of melt transport, and  
 51 the history of ice sheet growth and retreat.

52 Global data sets of the number of volcanic eruptions throughout the Pleistocene  
 53 would suggest there is a correlation between climatic change and volcanism (Huybers  
 54 & Langmuir, 2009), yet data resolution makes testing this association difficult. It is thought  
 55 that CO<sub>2</sub> and the trace element Nb have a relatively similar behaviour during decom-  
 56 pression melting (Saal, Hauri, Langmuir, & Perfit, 2002), and as such Nb compositions  
 57 can be used to gauge the quantity of CO<sub>2</sub> erupted. In Iceland there are just over 300 pub-  
 58 lished dated analysis of the Nb composition of Pleistocene lavas (Eason, Sinton, Grönvöld,  
 59 & Kurz, 2015; Gee, Taylor, Thirwall, & Murton, 1998). This is arguably the most com-  
 60 plete geochemical record of Nb compositions within a region that experienced significant  
 61 Pleistocene deglaciation. In this study we take a new approach, and use a high resolu-  
 62 tion model of ice sheet history to drive a forward model of melt generation and trans-  
 63 port, and predict CO<sub>2</sub> degassing. We validate the model predictions against the seismic  
 64 structure imaged below Iceland, and the observed crustal thickness. We subsequently  
 65 explore under what conditions climate and magmatism might be related, and the im-  
 66 plications for CO<sub>2</sub> degassing.

67 **2 Methods**

68 **2.1 Modelling of Melt Generation and Transport**

69 To investigate the impact of glacial activity on melt productivity, melt composition,  
 70 and CO<sub>2</sub> flux, we used a model of magma generation and transport coupled to a  
 71 model of the flexure of a viscoelastic beam for the response to change in load due to the  
 72 ice sheet history (see Supplementary Material). The coupled model consists of a flexural  
 73 model of the surface displacement due to the changing surface load as the ice sheet  
 74 changes in thickness. This model of surface displacement is then coupled to either a 1D  
 75 vertical column or a 2D corner flow model where the flow of the mantle is prescribed at  
 76 either an upwelling rate of 10 or 20 mm yr<sup>-1</sup>, or lateral spreading rate of 10 mm yr<sup>-1</sup>. We  
 77 use these two upwelling rates to cover the uncertainty in the exact rate of vertical as-  
 78 cent the mantle below Iceland due to mantle buoyancy. The upwelling column is per-  
 79 turbed by the displacement due to loading, where the viscoelastic decay time of the load  
 80 is set to 1000 yrs. Carbon partitioning into the melt is assumed to be governed by the  
 81 coefficients derived by (Rosenthal et al., 2015). We use a mantle source composition for  
 82 Nb of 1.627 ppm, which is intermediate between the end-member sources for Icelandic  
 83 melts identified by (Shortle & MacLennan, 2011). To approximate the melting of the mul-  
 84 tiple source lithologies we chose a solidus-depletion gradient of 600 °C which is interme-  
 85 diate between that of melting experiments on depleted mantle, 900 °C (Wasylewski, Baker,  
 86 Kent, & Stopler, 2003) and fertile mantle 300 °C (Scott, 1992).

87 The surface expression of partial melting to glacial loading/unloading is influenced  
 88 primarily by the rate at which the melt percolates through the mantle (Burley & Katz,  
 89 2015). To constrain the permeability of melt transport, we examined the effects of vary-  
 90 ing the permeability coefficient on the seismic properties of the mantle produced by our  
 91 1-D model. The thermal structure and porosity was converted to S-wave velocities, as-  
 92 suming that melt reduces the velocity by 7.9 % per percent porosity (Hammond & Humphreys,  
 93 2000) and including the effects of attenuation (Goes, Armitage, Harmon, Huismans, &  
 94 Smith, 2012). Recent joint inversion of teleseismic and ambient noise Rayleigh waves in  
 95 Iceland would suggest that the S-wave velocity is between 4 and 3.8 km s<sup>-1</sup> at depths  
 96 of 50 to 150 km (Harmon & Rychert, 2016) (Figure 1). We find that the permeability  
 97 coefficient,  $k_0$ , needs to be relatively high ( $10^{-5}$  m<sup>2</sup>) giving a permeability,  $k_\phi = k_0 \phi^3$   
 98 (where  $\phi$  is porosity), of the order of  $10^{-14}$  m<sup>2</sup> ( $\phi \approx 0.001$ ; Figure 1), because other-  
 99 wise porosity would be too large and the S-wave velocity would decrease below the ob-  
 100 served values. This permeability is an order of magnitude higher than the upper range  
 101 used to explore how sea-level change might influence mid-ocean ridge (MOR) magma-  
 102 tism (Burley & Katz, 2015; Crowley et al., 2015), and suggests rates of magmatic ascent  
 103 of the order of 10 m yr<sup>-1</sup>, in agreement with MacLennan et al. (2002). Previously it has  
 104 been suggested that delays in signal propagation from the zone of partial melting at MORs  
 105 to the surface might be of the order of a Milankovitch-scale period, 40 kyr (Huybers &  
 106 Langmuir, 2017). However, the high permeability required to match the seismic obser-  
 107 vations from Iceland implies a magmatic system that much more rapidly responds to change  
 108 in melting conditions, consistent with the fast transport rates estimated from U-series  
 109 isotope studies (Elliot & Spiegelman, 2014).

110 **2.2 Glacial Forcing Throughout the Pleistocene**

111 Iceland experienced extensive ice-cover during the last glacial period (Patton, Hub-  
 112 bard, Bradwell, & Schomackere, 2017), with maximum thicknesses in the center of the  
 113 island of ~ 2km attained by ~23 ka (Figure 2a and b). Deglaciation after the LGM oc-  
 114 curred at a varying rate, and was discontinuous. For example, a stage of re-advance oc-  
 115 curred during the colder climate of the Younger Dryas (11.7-12.9 ka) (Nordahl & Ingólfsson,  
 116 2015). The final phase of deglaciation was particularly rapid, with the main volcanic zones  
 117 being largely ice free by ~10 ka (Figure 2a). The most uncertain period of the glacial

history is the pre-LGM growth of the ice sheet. To create the ice sheet histories shown in Figure 2b and Figure 3a we calibrated the ice volume since the LGM against the North Greenland Ice Core Project (NGRIP)  $\delta^{18}\text{O}$  record, and Quaternary sea-level curves assuming a linear correlation between these three signals (see Supplementary Material Text S1). We focus on two scenarios: M1, based on the ICE-5G sea-level curves (Peltier, 2004), and M2, based on the sea-level curves of Pico, Creveling, and Mitrovica (2017) (Figure S2).

### 3 Results

#### 3.1 Effect of glacial loading and unloading

We force our melt model with the 120 ka glacial history after a 5 Myr model wind-up to steady state (model M1, Figure 2b) and using a single value for the ice thickness at each time-step, therefore neglecting the effects of the distal parts of the ice sheet on melting beneath the rift margins. The model predicts peaks in magmatic output and  $\text{CO}_2$  flux as pressure changes due to loading and unloading impact the melt production rate (Figure 2). The response of the magmatic system to changes in ice cover varies depending on the mantle upwelling rate, the rate-of-change in ice sheet thickness, and the prior ice sheet history. Glacial loading suppresses melt production (Jull & McKenzie, 1996), leading to a decline in magma supply (see Supplementary Material, Figure S3). For example during the period between 35 and 15 ka, the growth of the ice sheet reduces eruption rates below 5 km of melt per Myr (Figure 2c). The recovery from this loading occurs initially in the deepest part of the system as this region is perturbed the least. Recovery is also faster if the mantle upwelling rate is higher, where an upwelling rate of  $20 \text{ mm yr}^{-1}$  is more responsive than the equivalent  $10 \text{ mm yr}^{-1}$  model (Figure 2b). Higher rates of change in surface loading will impact melt production more strongly such that small magnitude but rapid deglaciation events, for example at  $\sim 85$  ka, have a relatively large effect on eruption rates (Figure 2c).

The impact of deglaciation events is modulated by the upwelling rate of the solid mantle because the upwelling rate controls the background productivity of the melting model. At slower upwelling rates, i.e.  $10 \text{ mm yr}^{-1}$ , some periods of deglaciation are not recorded in the flux of magma erupted. An example of this is the warming event at 60 ka (Figure 2), where the  $10 \text{ mm yr}^{-1}$  upwelling model produces no response in either the eruption rate or  $\text{CO}_2$  flux. If however upwelling is more rapid,  $20 \text{ mm yr}^{-1}$ , then there is a clear pulse in melt eruption rate (Figure 2). For a more productive scenario, there is increased shallow melting. The displacement imposed by the flexural response to unloading dissipates with depth. Therefore, if melting is productive and hence shallow it will feel the effects of the unloading to a greater extent when compared to a less productive melting system. Furthermore, when productivity is low, the porosity is low and the rate of vertical melt flow is slow such that a pulse in melt production will not reach the surface rapidly.

The magnitude of  $\text{CO}_2$  flux peaks are not linearly related to the magnitude in eruption rates (Figure 2d). For example, in the  $20 \text{ mm yr}^{-1}$  upwelling rate model, the largest  $\text{CO}_2$  peak is estimated to occur at  $\sim 60$  ka and not during the volumetrically larger magmatic pulse at the end of the Pleistocene (Figure 2d). This difference is because when the  $\sim 60$  ka warming occurred, the melt was enriched in carbon due to the preceding rapid glaciation. Magma supplied from the mantle during the Late-Pleistocene pulse were more depleted in carbon compared to those in the 60 ka event. The implication of this result is that volumetrically small volcanic events might have just as a strong influence on  $\text{CO}_2$  degassing as the more significant periods of volcanic eruptions, and the magnitude of  $\text{CO}_2$  degassing is dependent on the history of glacial forcing.

167      **3.2 Glacial Forcing Through the Latest Pleistocene and Holocene**

168      During the last 40 ka, our model suggest that CO<sub>2</sub> flux is highly dependent on the  
 169      glacial forcing. There are two distinct late Pleistocene magmatic pulses, separated by  
 170      the Younger Dryas cold period (Figure 3a and b). However, for the model M2 ice sheet  
 171      history there are three pulses in CO<sub>2</sub> flux at the end of the Pleistocene, due to the faster  
 172      ice sheet growth entering the LGM from 35 to 25 ka in this model (Figure 3a and e). This  
 173      peak in CO<sub>2</sub> flux is because the small magnitude but rapid deglaciations after 25 ka tap  
 174      melts rich in trace elements including Nb and carbon (Figure 3c and d).

175      The observed time series of incompatible trace element concentrations in Icelandic  
 176      magmas and ice sheet history have been suggested to be strongly associated (Eason et  
 177      al., 2015; Gee et al., 1998; Jull & McKenzie, 1996; MacLennan et al., 2002; Sinton et al.,  
 178      2005). Of these studies Gee et al. (1998) and Eason et al. (2015) report on the Nb com-  
 179      position of lavas erupted and give age ranges for the erupted lavas. Dating lava flow in  
 180      Iceland is complex given the lack of reliable markers from which ages can be obtained.  
 181      This means that ages are instead typically taken from the morphology and tephrochronol-  
 182      ogy of erupted flows (MacLennan et al., 2002), which is subjective and open to debate.  
 183      We therefore must take the age ranges for the Nb compositions reported by Gee et al.  
 184      (1998) and Eason et al. (2015) as indicative. We therefore chose to bin the ages into 2.5 kyr  
 185      intervals from 0 to 17.5 ka and then at 5 kyr intervals (Figure 3c). The reduction in Nb  
 186      compositions plotted is in line with the trends observed within the more selective La and  
 187      Sm data set presented in MacLennan et al. (2002), and is therefore likely robust.

188      We find that the predicted change in Nb from all our models fits within the range  
 189      of the observations (Figure 3c). The M2 model gives the strongest signature in Nb con-  
 190      centrations of deglaciation during the end of the Pleistocene, while the signature is more  
 191      subdued in the M1 ice sheet model (Figure 3c). The 1D forward model used is highly  
 192      idealised, and yet the agreement between the observations and model is encouraging, and  
 193      suggests the compositional change observed in lavas erupted during the late-Pleistocene  
 194      to early Holocene is due to rapid deglaciation (Eason et al., 2015; Gee et al., 1998; Maclen-  
 195      nan et al., 2002; Sinton et al., 2005). This implies that the observed change in melt com-  
 196      position is due to change in ice sheet loading and that the pre-deglaciation volcanism  
 197      likely released a significant volume of CO<sub>2</sub> (Figure 3e).

198      The 1D column model will underestimate the impact of change in deep melt pro-  
 199      ductivity, as it cannot capture the deep wings of the zone of partial melting. To explore  
 200      the impact of this we force a series of 1D models with the vertical flow taken from steady  
 201      state corner flow perturbed by the flexural response of the deglaciation of a 200 km wide  
 202      ice sheet. The half spreading rate is assumed to be 10 mm yr<sup>-1</sup>, and the mantle poten-  
 203      tial temperature is 1450 °C. Melt travels vertically from the zone of partial melting in  
 204      columns at 0 to 80 km from the rift axis (Figure 4). The steady state thickness of melt  
 205      erupted at the surface of the simplified 2D model is 15 km (Figure S4), and glacial forc-  
 206      ing causes this thickness to vary around this value by the order of 10 km except for a large  
 207      spike at the LGM. The crust of Iceland varies in thickness from 20 to 40 km (e.g. Jenk-  
 208      ins et al., 2018), and therefore a model steady state thickness of 15 km is a reasonable  
 209      lower end-member prediction given that the crust is made of both extrusions and intru-  
 210      sions.

211      After glacial perturbation we find that in the central zone, from the ridge centre  
 212      to 40 km distance, the trend in Nb and CO<sub>2</sub> flux is relatively similar, with a reduction  
 213      in Nb at 15 ka. At distances greater than 40 km, a peak in Nb and CO<sub>2</sub> flux is predicted  
 214      to occur with an increasing delay compared to the centre of extension (Figure 4). This  
 215      delay is due to the greater distance that the melt has to travel along the vertical path  
 216      from the top of the melt zone to the surface at increasing distance from the centre of ex-  
 217      tension. In full 2D models the distal melt will pool as it migrates laterally towards the  
 218      centre of extension (Katz, 2008), yet the difference in ascent velocity due to the increase

219 porosity as the melt pools would likely not be sufficient to overcome the increased dis-  
220 tance that the signal will have to travel.

221 The full solution to the coupled equations of magma dynamics would suggest that  
222 melts generated at a distance of up to 60 km from the centre of extension are advected  
223 to the ridge axis (Katz, 2008). If all of the melt generated up to 60 km from the centre  
224 of extension is erupted, then the CO<sub>2</sub> flux is significantly increased during the Holocene  
225 due to the addition input of melt from the distal parts of the zone of partial melting (Fig-  
226 ure 4b). Therefore these low productivity and deep regions of the zone of partial melt-  
227 ing might be a key exporter of mantle carbon into the atmosphere. However, the range  
228 of observed Nb concentrations are relatively similar to the axial concentrations, from within  
229 <40 km of the rift centre (Figure 4). This would suggest that the widest regions of the  
230 zone of partial melting are not sampled by the volcanism in the Reykjanes Ridge and  
231 Western Volcanic Zone, leading to an estimate of CO<sub>2</sub> fluxes more in line with the sim-  
232 pler 1D model.

#### 233 4 Discussion and Conclusions

234 The models imply that the deglaciation beginning at 18 ka and continuing through  
235 the Bolling warming at 14.8 ka released substantial quantities of CO<sub>2</sub> when compared  
236 to the last 120 ka (Figure 3c and Figure 4b), and this elevated CO<sub>2</sub> release was because  
237 of the preceding growth of the ice sheet. Volcanism during this time would have taken  
238 place in a sub-glacial environment and unsurprisingly does not feature in the post-glacial  
239 sub-aerial record. Evidence from sub-glacial volcanic units (tuyas) erupted during this  
240 time period (Hartley, Thordarson, & de Joux, 2016) suggest volumetric and composi-  
241 tional trends consistent with those predicted by our model (Figure 3c and Figure 4).

242 Forcing our model with the long-term 120 ka ice sheet history produces a periodic  
243 fluxing of CO<sub>2</sub> from Icelandic volcanoes due to ice-loss events over this period, implying  
244 a close link between ice dynamics and magmatic out-gassing. The greatest release  
245 of CO<sub>2</sub>, however, occurred during the period of ice-loss just before the Younger Dryas  
246 (~14 ka), and therefore before the largest phase of late-Pleistocene deglaciation (Figure  
247 4). The concentration of CO<sub>2</sub> released in this magmatic pulse was enhanced due to the  
248 lack of any significant loss of ice volume since ~40 ka. This created a magmatic system  
249 capable of fluxing large volumes of carbon during the initial period of post-LGM deglacia-  
250 tion (both models M1 and M2, Figure 3e), possibly contributing to the increased atmo-  
251 spheric CO<sub>2</sub> levels thought to be recorded between 15 and 14 ka in the EPICA Dome C  
252 ice core (Köhler, Knorr, Buiiron, Lourantou, & Chappellaz, 2011). It is therefore possi-  
253 ble that this pulse of magmagenic CO<sub>2</sub>, from Iceland and elsewhere (e.g. /citephuybers-  
254 2009, bolstered the climate warming, and final phase of deglaciation, that proceeded the  
255 Younger Dryas.

256 The CO<sub>2</sub> flux due to deglaciation is strongly influenced by the ice sheet history.  
257 Mantle CO<sub>2</sub> flux does not follow a linear relationship with eruption rates: large peaks  
258 in CO<sub>2</sub> are also predicted for periods in time when the volume flux is not very high (Fig-  
259 ure 2d and 3e). In effect we cannot conclude that all deglaciation events, or other rapid  
260 unloading events due to for example erosion (e.g. Sternai, Caricchi, Castelltort, & Cham-  
261 pagnac, 2016), lead to a large flux of volatile gases into the Earths atmosphere. The Earth  
262 system is more complex than such simple causality, yet one clear implication is that deglaci-  
263 ation after a prolonged period of ice-house conditions will lead to a significant carbon de-  
264 gassing of the upper mantle.

#### 265 Supporting Information

266 A detailed discussion of the methodology can be found in the supporting informa-  
267 tion (Andersen et al., 2004; Andrews, 2008; Armitage, Collier, Minshull, & Henstock, 2011;

268 Clark et al., 2009; Geirsdóttir, 2011; Gibson & Geist, 2010; Gurenko & Chaussidon, 1995;  
 269 Katz, Spiegelman, & Langmuir, 2003; Lambeck & Chappel, 2001; Lambeck, Rouby, Pur-  
 270 cell, Sun, & Sambridge, 2014; McKenzie & O’Nions, 1991; Miller, Zhu, Montési, & Gae-  
 271 tani, 2014; Ribe, 1985; Scott, 1992; Shorttle & MacLennan, 2011; Silbeck, 1975; Sleep &  
 272 Snell, 1976; Spiegelman, 1996; Spratt & Lisicki, 2016).

### 273 Acknowledgments

274 We would like to thank M. A. Mary Gee (The University of Western Australia) for shar-  
 275 ing her Nb composition data from the Reykjanes Peninsula, and Tamara Pico (Harvard  
 276 University) for sharing her sea level curves. John J. Armitage acknowledges funding from  
 277 an Agence National de la Recherche (France), Accueil de Chercheurs de Haute Niveau,  
 278 grant InterRift. The 1-D melting model is available from <https://bitbucket.com/johnjarmitage/melt1d-icesheet/>

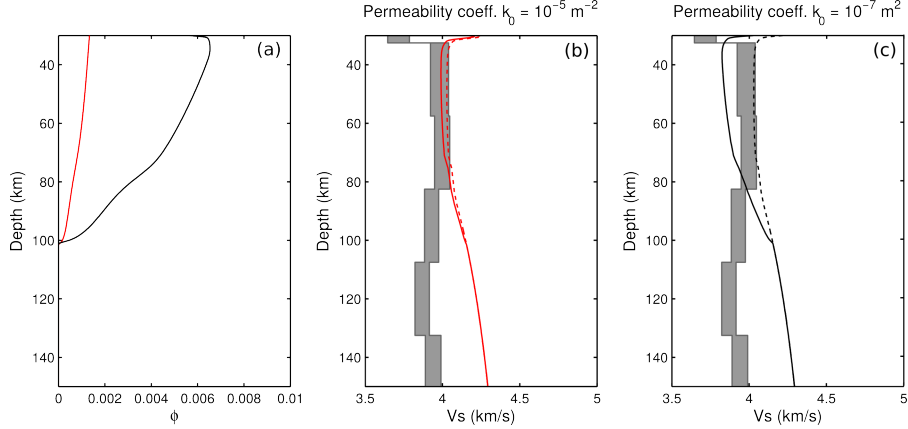
### 280 References

- 281 Andersen, K. K., Azuma, N., Barnola, J. M., Bigler, M., Biscaye, P., Caillon, N.,  
 282 ... White, J. W. C. (2004). High-resolution record of northern hemisphere  
 283 climate extending into the last interglacial period. *Nature*, *431*, 174-151. (doi:  
 284 10.1038/nature02805)
- 285 Andrews, J. T. (2008). The role of the Iceland Ice Sheet in the North Atlantic dur-  
 286 ing the late Quaternary: a review and evidence from Denmark Strait. *Journal*  
 287 *of Quaternary Science*, *23*, 3-20. (doi: 10.1002/jqs.1142)
- 288 Armitage, J. J., Collier, J. S., Minshull, T. A., & Henstock, T. J. (2011). Thin  
 289 oceanic crust and flood basalts: India-Seychelles breakup. *Geochemistry Geo-  
 290 physics Geosystems*, *12*(Q0AB07). (doi:10.1029/2010GC003316)
- 291 Burley, J. M. A., & Katz, R. F. (2015). Variations in mid-ocean ridge CO<sub>2</sub> emis-  
 292 sions driven by glacial cycles. *Earth and Planetary Science Letters*, *426*, 246-  
 293 258. (doi: 10.1016/j.epsl.2015.06.031)
- 294 Clark, P. U., Dyle, A. S., Shakun, J. D., Carlson, A. E., Clark, J., Wohlfarth, B., ...  
 295 McCabe, A. M. (2009). The last glacial maximum. *Science*, *325*, 710. (doi:  
 296 10.1126/science.1172873)
- 297 Crowley, J. W., Katz, R. F., Huybers, P., Langmuir, C. H., & Park, S. H. (2015).  
 298 Glacial cycles drive variations in the production of oceanic crust. *Science*, *347*,  
 299 1237-1240. (doi: 10.1126/science.1261508)
- 300 Dasgupta, R., & Hirschmann, M. M. (2010). The deep carbon cycle and melting  
 301 in Earth’s interior. *Earth and Planetary Science Letters*, *298*, 1-13. (doi:  
 302 10.1016/j.epsl.2010.06.039)
- 303 Eason, D. E., Sinton, J. M., Gronvöld, K., & Kurz, M. D. (2015). Effects of  
 304 deglaciation on the petrology and eruptive history of the Western Volcanic  
 305 Zone, Iceland. *Bulletin of Volcanology*, *77*(47). (doi: 10.1007/s00445-015-0916-  
 306 0)
- 307 Elliot, T., & Spiegelman, M. (2014). Melt migration in oceanic crustal production:  
 308 A u-series perspective. In *Treatise on geochemistry* (2nd ed., p. 543-581). Else-  
 309 vier. (doi: 10.1016/B978-0-08-095975-7.00317-X)
- 310 Gee, M. A. M., Taylor, R. N., Thirwall, M., & Murton, B. J. (1998). Glacioisostacy  
 311 controls chemical and isotopic characteristics of tholeiites from the Reykjanes  
 312 Peninsula, SW Iceland. *Earth and Planetary Science Letters*, *164*, 1-5.
- 313 Geirsdóttir, A. (2011). Pliocene and pleistocene glaciations of iceland: a brief  
 314 overview of the glacial history. In J. Ehlers, P. L. Gibbard, & P. Hughes  
 315 (Eds.), *Quaternary glaciations - extent and chronology, a closer look* (Vol. 15,  
 316 p. 199-210). Elsevier. (doi: 10.1016/B978-0-444-53447-7.00016-7)
- 317 Gibson, S. A., & Geist, D. (2010). Geochemical and geophysical estimates of litho-  
 318 spheric thickness variation beneath galápagos. *Earth and Planetary Science*

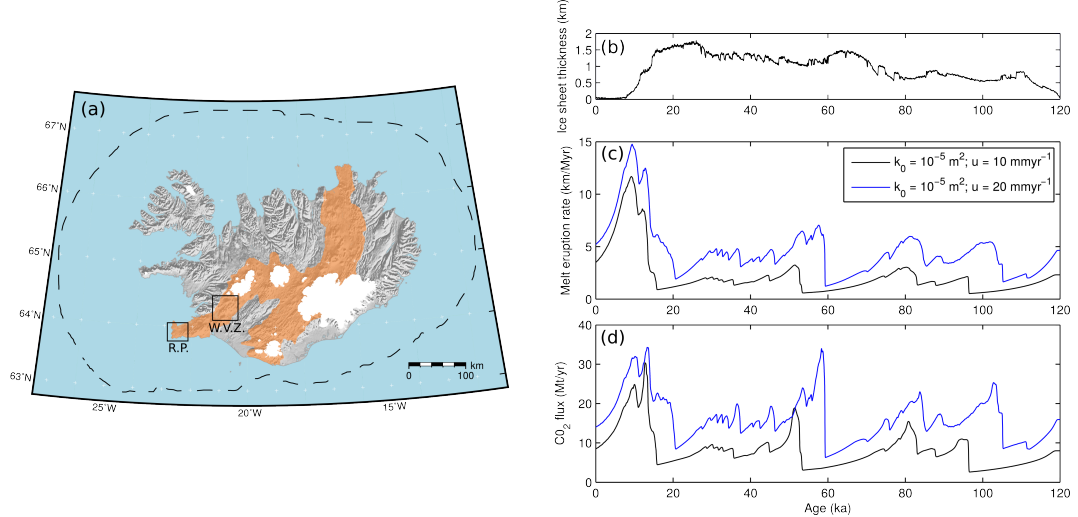
- Letters, 300, 275-286. (doi: 10.1016/j.epsl.2010.10.002)
- Glazner, A. F., Manley, C. R., Marron, J. S., & Rojstaczer, S. (1999). Fire or ice: Anticorrelation of volcanism and glaciation in California over the past 800,000 years. *Geophysical Research Letters*, 26, 1759-1762. (doi: 10.1029/1999GL900333)
- Goes, S., Armitage, J. J., Harmon, N., Huismans, R., & Smith, H. (2012). Low seismic velocities below mid-ocean ridges: Attenuation vs. melt retention. *Journal of Geophysical Research*, 117, B12403. (doi: 10.1029/2012JB009637)
- Gureenko, A. A., & Chaussidon, M. (1995). Enriched and depleted primitive melts included in olivine from Icelandic tholeiites: Origin by continuous melting of a single mantle column. *Geochimica et Cosmochimica Acta*, 59, 2905-2917.
- Hammond, W. C., & Humphreys, E. D. (2000). Upper mantle seismic wave velocity: Effects of realistic partial melt geometries. *Journal of Geophysical Research*, 105, 10975-10986.
- Harmon, N., & Rychert, C. A. (2016). Joint inversion of teleseismic and ambient noise Rayleigh waves for phase velocity maps, an application to Iceland. *Journal of Geophysical Research*, 121, 5966-5987. (doi: 10.1002/2016JB012934)
- Hartley, M. E., Thordarson, T., & de Joux, A. (2016). Postglacial eruptive history of the Askja region, North Iceland. *Bulletin of Volcanology*, 78(28). (doi: 10.1007/s00445-016-1022-7)
- Huybers, P., & Langmuir, C. H. (2009). Feedback between deglaciation, volcanism, and atmospheric CO<sub>2</sub>. *Earth and Planetary Science Letters*, 286, 479-491. (doi: 10.1016/j.epsl.2009.07.014)
- Huybers, P., & Langmuir, C. H. (2017). Delayed CO<sub>2</sub> emissions from mid-ocean ridge volcanism as a possible cause of late-Pleistocene glacial cycles. *Earth and Planetary Science Letters*, 457, 238-249. (doi: 10.1016/j.epsl.2016.09.021)
- Jellinek, M. A., Mange, M., & Saar, M. O. (2004). Did melting glaciers cause volcanic eruptions in eastern California? probing the mechanisms of dike formation. *Journal of Geophysical Research*, 109(B09206). (doi: 10.1029/2004JB002978)
- Jenkins, J., MacLennan, J., Green, R. G., Cottaar, S., Deuss, A. F., & White, R. S. (2018). Crustal formation on a spreading ridge above a mantle plume: Receiver function imaging of the Icelandic crust. *Journal of Geophysical Research*, 123, 5190-5208. (doi: 10.1029/2017JB015121)
- Jull, M., & McKenzie, D. (1996). The effect of deglaciation on mantle melting beneath Iceland. *Journal of Geophysical Research*, 101(B10), 21815-21828.
- Katz, R. F. (2008). Magma dynamics with the enthalpy method: Benchmark solutions and magmatic focusing at mid-ocean ridges. *Journal of Petrology*, 49, 2099-2121. (doi:10.1093/petrology/egn058)
- Katz, R. F., Spiegelman, M., & Langmuir, C. H. (2003). A new parameterization of hydrous mantle melting. *Geochemistry Geophysics Geosystems*, 4, 1073. (doi: 10.1029/2002GC000433)
- Köhler, P., Knorr, G., Buiron, D., Lourantou, A., & Chappellaz, J. (2011). Abrupt rise in atmospheric CO<sub>2</sub> at the onset of the Bolling/Allerod: in-situ ice core data versus true atmospheric signals. *Climate of the Past*, 7, 473-486. (doi: 10.5194/cp-7-473-2011)
- Lambeck, K., & Chappel, J. (2001). Sea level change through the last glacial cycles. *Science*, 292, 679-686. (doi: 10.1126/science.1059549)
- Lambeck, K., Rouby, H., Purcell, A., Sun, Y., & Sambridge, M. (2014). Sea level and global ice volumes from the Last Glacial Maximum to the Holocene. *Proceedings of the National Academy of Sciences*, 111, 15296-15303. (doi: 10.1073/pnas.141176211)
- Lund, D. C., & Asimow, P. D. (2011). Does sea level influence mid-ocean ridge magmatism on Milankovitch timescales? *Geochemistry Geophysics Geosystems*, 12(Q12009). (doi: 10.1029/2011GC003693)

- 374 Maclennan, J., Jull, M., McKenzie, D., Slater, L., & Gronvöld, K. (2002). The  
 375 link between volcanism and deglaciation in Iceland. *Geochemistry Geophysics  
 376 Geosystems*, 3(11, 1062). (doi: 10.1029/2001GC000282)
- 377 McKenzie, D., & O'Nions, R. K. (1991). Partial melt distribution from inversion of  
 378 rare earth element concentrations. *Journal of Petrology*, 32, 1021-1091.
- 379 Miller, K. J., Zhu, W., Montési, L. G. J., & Gaetani, G. A. (2014). Experimental  
 380 quantification of permeability of partially molten mantle rock. *Earth and Plan-  
 381 etary Science Letters*, 388, 273-282. (doi: 10.1016/j.epsl.2013.12.003)
- 382 Nordahl, H., & Ingólfsson, O. (2015). Collapse of the Icelandic ice sheet controlled  
 383 by sea level rise? *Arktos*, 1, 1-13. (doi: 10.1007/s41063-015-0020-x)
- 384 Pagli, C., & Sigmundsson, F. (2008). Will present day glacier retreat increase  
 385 volcanic activity? stress induced by recent glacier retreat and its effect on  
 386 magmatism at the Vatnajökull ice cap, Iceland. *Geophysical Research Letters*,  
 387 35(L09304). (doi: 10.1029/2008GL033510)
- 388 Patton, H., Hubbard, A., Bradwell, T., & Schomackere, A. (2017). The configura-  
 389 tion, sensitivity and rapid retreat of the Late Weichselian Icelandic ice sheet.  
 390 *Earth-Science Reviews*, 166, 223-245. (doi: 10.1016/j.earscirev.2017.02.001)
- 391 Peltier, W. R. (2004). Global glacial isostacy and the surface of the ice-age Earth:  
 392 The ICE-5G (VM2) model and grace. *Annual Reviews of Earth and Planetary  
 393 Science*, 32, 111-149. (2004)
- 394 Pico, T., Creveling, J. R., & Mitrovica, J. X. (2017). Sea-level records from the  
 395 U.S. mid-Atlantic constrain Laurentide Ice Sheet extent during Marine Isotope  
 396 Stage 3. *Nature Communications*, 8(15621). (doi: 10.1038/ncomms15612)
- 397 Rawson, H., Pyle, D. M., Mather, T. A., Smith, V. S., Fontjin, K., Lachowycz,  
 398 S. M., & Naranjo, J. A. (2016). The magmatic and eruptive response of arc  
 399 volcanoes to deglaciation: Insights from southern Chile. *Geology*, 44, 251-254.  
 400 (doi: 10.1130/G37504.1)
- 401 Ribe, N. M. (1985). The generation and composition of partial melts in the earth's  
 402 mantle. *Earth and Planetary Science Letters*, 73, 361-376.
- 403 Rosenthal, A., Hauri, E. H., & Hirschmann, M. M. (2015). Experimental determi-  
 404 nation of C, F, and H partitioning between mantle minerals and carbonated  
 405 basalt, CO<sub>2</sub>/Ba and CO<sub>2</sub>/Nb systematics of partial melting, and the CO<sub>2</sub>  
 406 contents of basaltic source regions. *Earth and Planetary Science Letters*, 415,  
 407 77-87. (doi: 10.1016/j.epsl.2014.11.044)
- 408 Saal, A. E., Hauri, E. H., Langmuir, C. H., & Perfit, M. R. (2002). Vapour un-  
 409 dersaturation in primitive mid-ocean-ridge basalt and the volatile content of  
 410 Earths upper mantle. *Nature*, 419, 451-455. (doi: 10.1038/nature01073)
- 411 Schmidt, P., Lund, B., Hieronymus, C., MacLennan, J., Arnadottir, T., & Pagli,  
 412 C. (2013). Effects of present-day deglaciation in Iceland on mantle melt  
 413 production rates. *Journal of Geophysical Research*, 118, 3366-3379. (doi:  
 414 10.1002/jgrb.50273)
- 415 Scott, D. R. (1992). Small-scale convection and mantle melting beneath mid-ocean  
 416 ridges. In J. Phipps Morgan, D. K. Blackman, & J. M. Sinton (Eds.), *Mantle  
 417 flow and melt generation at mid-ocean ridges* (Vol. Geophysical Monograph 71,  
 418 p. 327-352). American Geophysical Union.
- 419 Shorttle, O., & MacLennan, J. (2011). Compositional trends of icelandic  
 420 basalts: Implications for short-length scale lithological heterogeneity in  
 421 mantle plumes. *Geochemistry Geophysics Geosystems*, 12, Q11008. (doi:  
 422 10.1029/2011GC003748)
- 423 Sigvaldsson, G. E., Annertz, K., & Nilsson, M. (1992). Effect of glacier load-  
 424 ing/delowering on volcanism: postglacial volcanic production rate of the Dyn-  
 425 gjufjöll area, central Iceland. *Bulletin of Volcanology*, 54, 385-392. (doi:  
 426 10.1007/BF00312320)
- 427 Silbeck, J. N. (1975). On the fluid dynamics of ridge crests. In *Notes on the 1975  
 428 summer study program in geophysical fluid dynamics at the Woods Hole Ocean-*

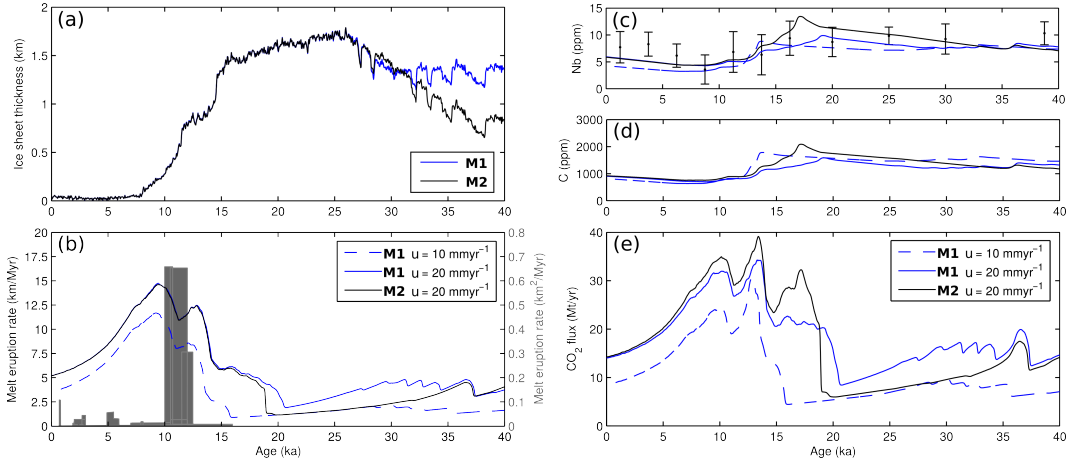
- 429       graphic institution, (Vol. 2, p. 113-122).
- 430     Sinton, J., Grönvold, K., & Saemundsson, K. (2005). Postglacial eruptive history  
431       of the Western Volcanic Zone, Iceland. *Geochemistry Geophysics Geosystems*,  
432       6(Q12006). (doi: 10.1029/2005GC001021)
- 433     Sleep, N. H., & Snell, N. S. (1976). Thermal contraction and flexure of mid-  
434       continent and Atlantic marginal basins. *Geophysical Journal of the Royal  
435       Astronomical Society*, 45, 125-154.
- 436     Spiegelman, M. (1996). Geochemical consequences of melt transport in 2-D: The  
437       sensitivity of trace elements to mantle dynamics. *Earth and Planetary Science  
438       Letters*, 139, 115-132.
- 439     Spratt, R. M., & Lisiecki, L. E. (2016). A late Pleistocene sea level stack. *Climate of  
440       the Past*, 12, 1079-1092. (doi: 10.5194/cp-12-1079-2016)
- 441     Sternai, P., Caricchi, L., Castelltort, S., & Champagnac, J. D. (2016). Deglaciation  
442       and glacial erosion: A joint control on magma productivity by con-  
443       tinental unloading. *Geophysical Research Letters*, 43, 1632-1641. (doi:  
444       10.1002/2015GL067285)
- 445     Wasylewski, L. E., Baker, M. B., Kent, A. J. R., & Stopler, E. M. (2003). Near-  
446       solidus melting of the shallow upper mantle: partial melting experiments on  
447       depleted peridotite. *Journal of Petrology*, 44, 116-1191.



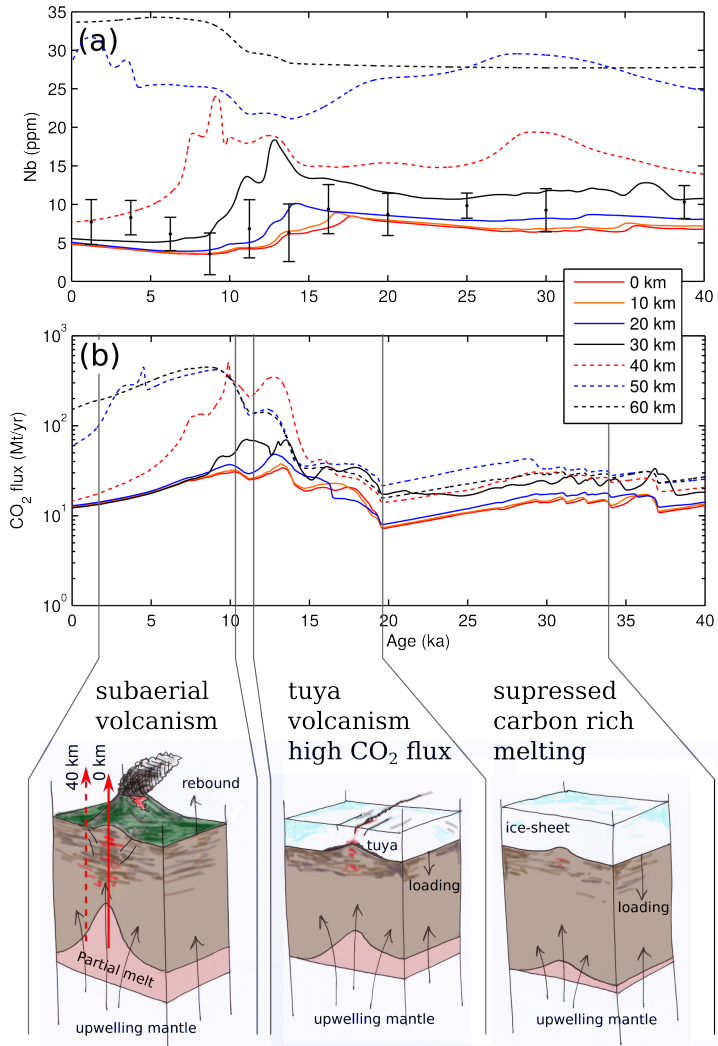
448 **Figure 1.** Profiles of porosity and S-wave seismic velocity for the two model permeabilities of  
449  $k_0 = 10^{-7} \text{ m}^2$  black line, and  $k_0 = 10^{-5} \text{ m}^2$  red line. (a) Porosity plotted against depth at steady  
450 state. (b) S-wave velocity from the joint inversion of teleseismic and ambient noise Rayleigh  
451 waves (Harmon & Rychert, 2016) and the predicted S-wave profile from the high permeability  
452 case. The model includes the addition of the adiabatic gradient, the anharmonic effects from the  
453 mineralogy and effects of attenuation (Goes et al., 2012). The dashed line assumes melt has no  
454 effect, the solid line includes a 7.9 % reduction in  $V_S$  per percent melt (Hammond & Humphreys,  
455 2000). (c) S-wave velocity predictions for the low permeability case.



456 **Figure 2.** Response of the model to periodic and observed ice sheet thickness changes of the  
457 last 120 ka. (a) Map of Iceland showing the locations of the volcanic rift zones in orange and the  
458 maximum extent of the ice sheet at the last glacial maximum (dashed line). The boxes show the  
459 location of the Reykjanes Peninsular (R. P.) and the Western Volcanic Zone (W. V. Z.). (b) The  
460 ice sheet thickness predicted from the ice sheet model M1 over the last 120 ka. (c) Melt eruption  
461 rate and (d) carbon flux response to the step change in ice sheet thickness: black line, an upper  
462 mantle permeability coefficient of  $k_0 = 10^{-5} \text{ m}^2$  and upwelling velocity of  $10 \text{ mm yr}^{-1}$ , and blue  
463 line, an upwelling velocity of  $20 \text{ mm yr}^{-1}$ .



464 **Figure 3.** Impact of ice sheet growth and decay on melt eruption and composition over the  
465 last 40 ka. (a) Ice sheet models M1 and M2 taken from the sea-level models of Peltier (2004) and  
466 Pico et al. (2017) respectively. (b) Melt eruption rates (in km of melt per Myr): blue solid line,  
467 ice sheet history 5G for  $k_0 = 10^{-5}$  m<sup>2</sup> with an upwelling rate of 20 mm yr<sup>-1</sup>; blue dashed line, M1  
468 for  $k_0 = 10^{-5}$  m<sup>2</sup> with an upwelling rate of 10 mm yr<sup>-1</sup>; black solid line, ice sheet history M2 for  
469  $k_0 = 10^{-5}$  m<sup>2</sup> with an upwelling rate of 20 mm yr<sup>-1</sup>. The gray region shows estimated eruption  
470 rates from geological observations (MacLennan et al., 2002)] (in km<sup>2</sup> of melt per Myr). (c) Ob-  
471 served and predicted Nb concentrations (ppm), observations are from the Reykjanes Peninsula  
472 and the Western Volcanic Zone (Eason et al., 2015; Gee et al., 1998; Sinton et al., 2005) and are  
473 binned at 2.5 kyr intervals from 0 to 17.5 ka and then at 5 kyr intervals. (d) Predicted variation of  
474 in the concentration of carbon (ppm) within the erupted melt. (e) Predicted variation in the flux  
475 of CO<sub>2</sub>, assuming that the flux of CO<sub>2</sub> that Icelandic volcanism covers an area of 30,000 km<sup>2</sup>, and  
476 CO<sub>2</sub> (ppm) = 3.67 C (ppm) (see Eq. 23 in the Supplementary Material).



477 **Figure 4.** Impact of glacial history on off-axis and on-axis melting. A series of 1D column  
 478 melting models forced by the response to deglaciation (ice sheet history model M1) where the  
 479 mantle flow is of steady state corner flow. (a) Nb concentrations from the centre of extension out  
 480 to 60 km from the centre of extension. The mean concentration weighted by the eruption rate is  
 481 plotted as the thick black line. (b) Predicted CO<sub>2</sub> flux from the series of vertical melting models.  
 482 The late-Pleistocene eruptions are typified by tuya magmatism. This will have been the case up  
 483 until at least ~14 ka, where either magmatism was suppressed or when eruptions occurred they  
 484 will have been beneath at least 1 km of ice-cover (Hartley et al., 2016). The suppressed melting  
 485 regime will have become carbon rich because the shallow low-C melt production is damped due  
 486 to the ice-sheet loading. Upon deglaciation there is increased volcanism, which initially taps the  
 487 melt rich carbon.